*Journal of Structural Geology*, Vol. 16, No. 1, pp. 11 to 20, 1994
Printed in Great Britain

0191-8141/94 $06.00+0.00


# East–west thrusting and anomalous magnetic declinations in the Sierra Gorda, Betic Cordillera, southern Spain

E. S. PLATZMAN*

Institüt für Geophysik, ETH Hönggerberg, CH 8093, Zürich Switzerland

(*Received* 10 *August* 1992; *accepted in revised form* 21 *January* 1993)

**Abstract**—Structural and palaeomagnetic studies in the Sierra Gorda (Sierra de Loja), located in the External zone of the Betic Cordillera, indicate that westward-directed thrusting is not associated with significant rotations about a vertical axis. Detailed mapping and slip vector analysis show that the Sierra Gorda is a thrust complex composed of three thrust sheets. The uppermost thrust places Early Jurassic pelagic carbonates on top of Jurassic to Oligocene sediments that form a large doubly-plunging footwall syncline. The eastern limb of this syncline has been overturned and is tectonically thinned as a result of the overthrusting.

Palaeomagnetic results from Mesozoic and Tertiary sediments both within and around the perimeter of the Sierra Gorda indicate that: (1) the average remanence vector of the seven Late Jurassic localities sampled within the Sierra Gorda has a direction ($D$ = 328° and $I$ = 38°) that is not significantly different from the expected declination for the Upper Jurassic of stable Iberia; and (2) there is no significant difference between the remanences in the two upper thrust sheets indicating that differential rotation did not occur during the initiation and displacement on the thrusts. In contrast, the one Late Jurassic site that was sampled to the west of the Sierra Gorda is rotated, like the rest of the Subbetics, 60° clockwise of the reference direction. The unrotated directions obtained in the Sierra suggest, either that it has rotated in a clockwise sense concordant with the rest of the Subbetic zone and has then been backrotated, or that it has never rotated relative to stable Iberia. In the latter, simpler hypothesis the unrotated declinations may be explained in terms of orthogonal convergence along an irregular continental margin.

## INTRODUCTION

THE Betic Cordillera of southern Spain lies at the western end of the Alpine–Mediterranean collisional system and forms the northern limb of the tightly curved Betic–Rif Arc. The Cordillera can be broadly divided into an Internal and an External zone based on structural and palaeogeographic criteria. The Internal zone is made up of Palaeozoic, Mesozoic and locally Tertiary rocks of the Alboran domain that were deformed and metamorphosed by pre-early Miocene Alpine orogenic events. The External zone comprises the Mesozoic and Tertiary sediments of the Iberian margin that were detached from their basement and shortened as a result of Miocene convergence between the Alboran domain and Iberia (Fig. 1). This collisional event has been interpreted as reflecting either the westward motion of an independent Alboran microplate (Andrieux *et al.* 1971, Leblanc & Olivier 1984, Boillin *et al.* 1986), or the post-collisional extensional collapse of the Alboran Domain (Garcia-Dueñas & Martinez 1988, Platt & Vissers 1989). In this context the faulted contact that separates the Internal and the External zones (IEZB) must be either a major dextral strike-slip fault or a thrust contact. Recent kinematics studies done along the eastern segment of this boundary (Lonergen *et al.* in press) suggest that displacement occurred on gently dipping thrust surfaces in a SE–SSE direction, oblique to its regional trend (070°), and hence support the compressional nature of the IEZB.

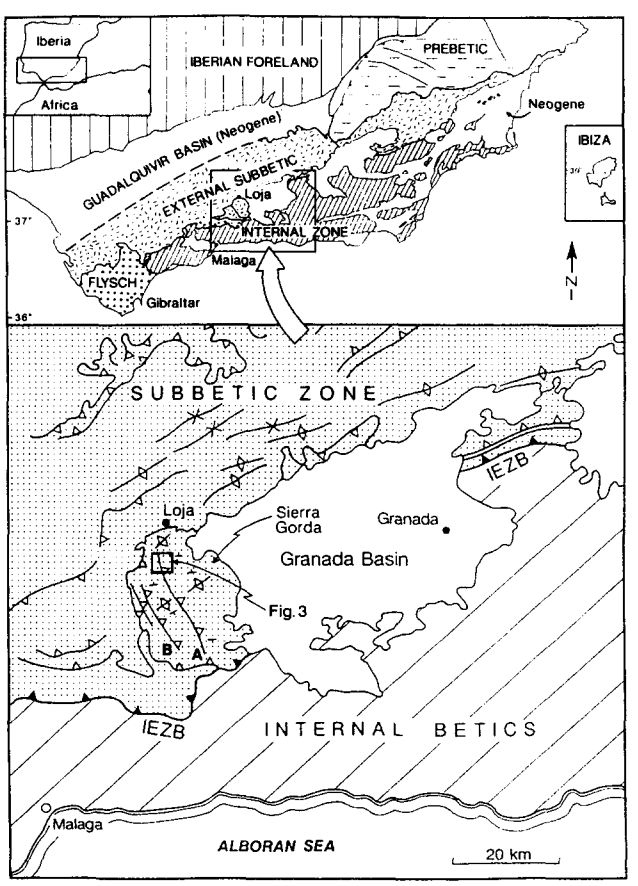


Fig. 1. Map showing regional and structural setting of the Sierra Gorda (based on the IGME Granada-Malaga, 1:200,000, geologic map). IEZB is Internal–External zone boundary shown with closes thrust symbols. Open thrust symbols used to denote smaller thrusts. A and B denote thrust surfaces discussed in the text.

*Current address; Department of Earth Sciences, Parks Road, Oxford OX1 3PR, U.K.

Palaeomagnetic data collected throughout much of the External zone (for example, Osete *et al.* 1988, 1989, Platzman & Lowrie 1992, Allerton *et al.* in review) show overwhelming evidence for substantial clockwise rotations. These data are generally compatible with the overall structure of the External zone in which foreland-directed thrusting (Garcia-Hernandez *et al.* 1980, Banks & Warburton 1991, Frizon de Lamotte *et al.* 1991) with a dextrally oblique component of motion (Platzman *et al.* 1991, Allerton *et al.* in review) is combined, in some areas, with wrench faulting (Paquet 1972, de Smet 1984, Hermes, 1988). Platzman (1992) suggests that both the general pattern of rotation and the structure of the External zone may be interpreted in terms of the interactions between an extending elongate Alboran domain with the passive margins of Africa and Iberia.

The Sierra Gorda, located in the External zone south of the town of Loja (Fig. 1), appears to be anomalous in several respects. Examination of a tectonic map of this region (Fig. 1) shows that the sierra has a NNW–SSE structural trend. This trend is distinct from the regional 070–090° trend in the central part of the External zone. The one previous palaeomagnetic study undertaken in the Sierra Gorda (Ogg *et al.* 1984) has also reported anomalous results. Ogg *et al.* (1984) studied a Late Jurassic (latest Oxfordian, Kimmeridgian and early Tithonian) carbonate section at Cortijo de Caldador for magnetostratigraphic purposes. In addition to the magnetostratigraphic sequence, Ogg *et al.* (1984) observed that the mean declination of the characteristic remanence vector at this locality is 324°, which is surprisingly different from those observed elsewhere in the Betic Cordillera. Osete *et al.* (1988) suggested that the anticlockwise rotation of the declination might be explained by either late Miocene left-lateral movement along the IEZB or a complex model of block rotations, such as the one described by Garfunkel & Ron (1985) in which adjacent blocks may exhibit rotations in opposing senses. The current study was designed to investigate the relationship between the apparently anomalous structure and rotation by: (a) defining the regional extent of the anomalous rotations; (b) seeing if the anomalous rotations correlate with anomalous transport directions or structures; and (c) seeing if differential rotations are related to distinct tectonic boundaries. To achieve this goal palaeomagnetic results from 10 additional sites both within and around the Sierra Gorda were integrated with data obtained from structural mapping and kinematic analysis, along selected contacts.

## GEOLOGICAL SETTING

The Sierra Gorda lies on the western edge of the Granada basin where the Internal–External zone boundary steps 20 km southward from the Sierra Arana, northeast of Granada, to the southern margin of the Sierra Gorda (Fig. 1). Blumenthal (1930, 1931) interpreted the Sierra Gorda as the westward continuation of the Penibetic palaeogeographic zone, which formed the southern submarine swell of the Subbetic during the Jurassic. More recent publications (Linares & Vera 1966, Vera 1969), however, consider this mountain as a separate unit known as the Unidad de Sierra Gorda. These authors maintain that the structure and the stratigraphy of the Sierra Gorda are sufficiently distinct from the remainder of the Subbetic to support such a subdivision.

The structure of the Sierra Gorda is discussed both in Vera (1969) and in the description accompanying the geologic map of Loja (Instituto Geologico y Mineron de España (IGME) 1989). Both of these publications describe the Sierra Gorda as a large N–S elongated domal structure that has been affected by a large number of faults. Vera (1969) believed that the regional structure was that of an anticline with the axis oriented E–W. He describes the inverted series observed along the axial zone of the Sierra Gorda and ascribes their geometry to a series of overturned folds verging SSE. He attributes this folding to southward-directed thrust faulting. Vera (1969) separates the faults observed in the Sierra Gorda into two groups. The first group of faults are those formed during folding. These faults are vertical and appear in conjugate pairs indicating a NNW–SSE maximal compression axis. The second group of faults reflects a phase of decompression. These normal faults trend WSW–ENE.

In contrast to Vera's (1969) original ideas, the text that accompanies the 1:50,000 geologic map of Loja (IGME 1989) states that the observed structure of the Sierra Gorda is the result of the superposition of two compressional phases of tectonism. The first of these tectonic phases formed southwestward-verging asymmetric anticlines with axes oriented N150°E. The normal flanks of these anticlines are on the order of kilometres in length while the overturned limbs are hectometres long. They observed that within the central axial zone of the mountain the normal flank of one of these anticlines is cut by a reverse fault. Like Vera (1969) they believe that this reverse fault is southward directed. The second phase of deformation formed folds with axes oriented N30–50°E.

## STRUCTURAL RESULTS

### *Kinematic analysis: principles and purpose*

In a region of brittle deformation such as the Sierra Gorda, slip surfaces often contain abundant sense of shear indicators. These features include wear grooves and striations, growth fibre lineations, gouge fabrics and Riedel shears. Some of these features record a unique direction and sense of motion while others only indicate a non-polar slip vector.

In most instances these slip vectors cannot be directly related either to stress or to the magnitude and direction of finite strain (Platt *et al.* 1988, Marrett & Allmendinger 1990, Twiss *et al.* 1991) but can provide a direction of an increment of relative displacement between two fault

blocks thereby providing critical information on the history of relative motion between individual components of the system. In addition, by defining the sense of motion on faults bounding discrete blocks these data can help the mechanism by which rotations might have occurred. Slip vector analysis in combination with information regarding rotations relative to a fixed reference frame can thus provide a more complete picture of the kinematic development of a deformed rock body.

*Slip vector analysis*

Slip vector data were collected along the major thrust contacts that trend roughly NNW through the Sierra Gorda (Fig. 1). Most of the data come from calcite fibre lineations, which often yield both a sense and a direction of relative displacement with respect to an adjacent rock body.

The results obtained from the axial thrust and the underlying one (A and B, Fig. 1) are presented in Figs. 2(a) & (b). Each equal-area stereonet shows a mean fault plane and the lineations that are associated with that set of surfaces. They show clearly that thrusting along both of these faults was in a WNW direction. The mean slip vector trends 110° and plunges 13° on very gently dipping surfaces, which include both eastward-dipping surfaces parallel to the main thrust fault, and westward-dipping surfaces parallel to a projected $R_1$ (Fig. 2c). These surfaces have a mean regional dip of approximately 20° to the east.

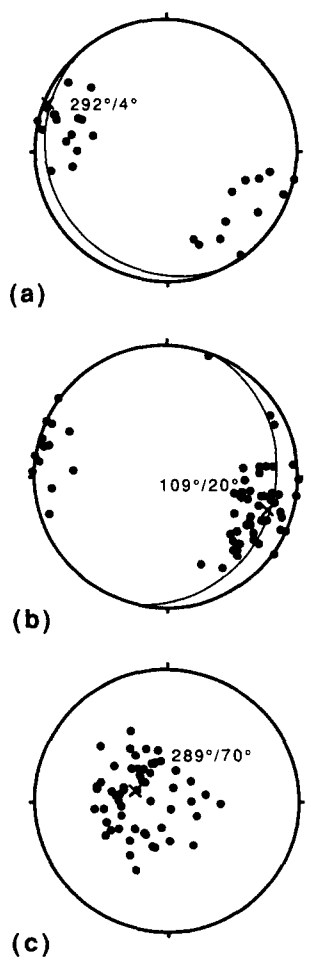


Fig. 2. Equal-area projections of structural data with mean vector ($X$) and orientation noted (a) lineations (dots) and mean slip surface from the axial fault zone (A in Fig. 1). (b) lineations (dots) and mean slip surface from fault zone B (Fig. 1). (c) Equal-area projection of the poles to the slip surfaces along the axial fault zone (A).

*The geometry of the axial thrust contact*

To examine the geometry of the upper thrust contact which crops out along the axial zone of the Sierra Gorda (Fig. 1) a detailed map (Fig. 3) was made along the northern segment of the fault where the footwall of this thrust is well exposed. The map shows that in the north, a major phase of WNW-directed thrusting has been superimposed on a gently northward-dipping (<30°) stratigraphic sequence. Because of its shallow dip, the outcrop pattern of this thrust fault is highly dependent on the topography. This can be clearly observed in the southern corner of the Las Cabras exposure.

Displacement along the thrust surface led to the formation of a footwall syncline. Equal-area plots of the poles to bedding show that the lithologic layering in these northern exposures is folded about an axis that plunges approximately 30° to 343–360° (Figs. 4a–c). The western limb of this footwall syncline is overturned and in many places tectonically thinned. The geometry of this syncline is illustrated in cross-section (B–B′) (Fig. 5) which shows a section constructed normal to the average fold axis.

Along the entire length of the axial fault zone, the main fault places the Liassic on top of the overturned limb of the footwall syncline. In the Alcantara exposure the fault places the Lower Liassic dolostones over the overturned limestones of the Upper Liassic. In the more southerly situated Las Cabras exposure, where the thrust is well exposed, it places Liassic limestones over the Liassic and the late Jurassic limestones of the overturned limb. Further to the south the thrust fault cuts progressively downwards into the N-dipping overturned limb of the footwall syncline. As a result it thrusts Liassic limestones on top of sequentially younger sediments. According to this line of reasoning the major axis of the early folding phase should be located where the thrust fault encounters the youngest (Oligocene) sediments. South of this boundary bedding dips generally southward and the thrust fault encounters progressively older sediments.

Associated with the thrust fault and the thrust-related syncline are many smaller scale structures (Fig. 3). Thrusts with a synthetic ($R_1$) orientation, although minor, are commonly present within the Late Jurassic or the Early Cretaceous sediments of the overturned limb.

In addition to thrust faults, normal faults are also present in this region. For example, normal faults that trend at a high angle to the direction of thrusting offset the Late Jurassic limestones of the normal limb in the Cuevas exposure. Listric normal faults in a similar orientation probably underlie the klippen observed in the Las Cabras exposure (Figs. 3 and 5). Finally, normal faults that trend at a lower angle to the direction of

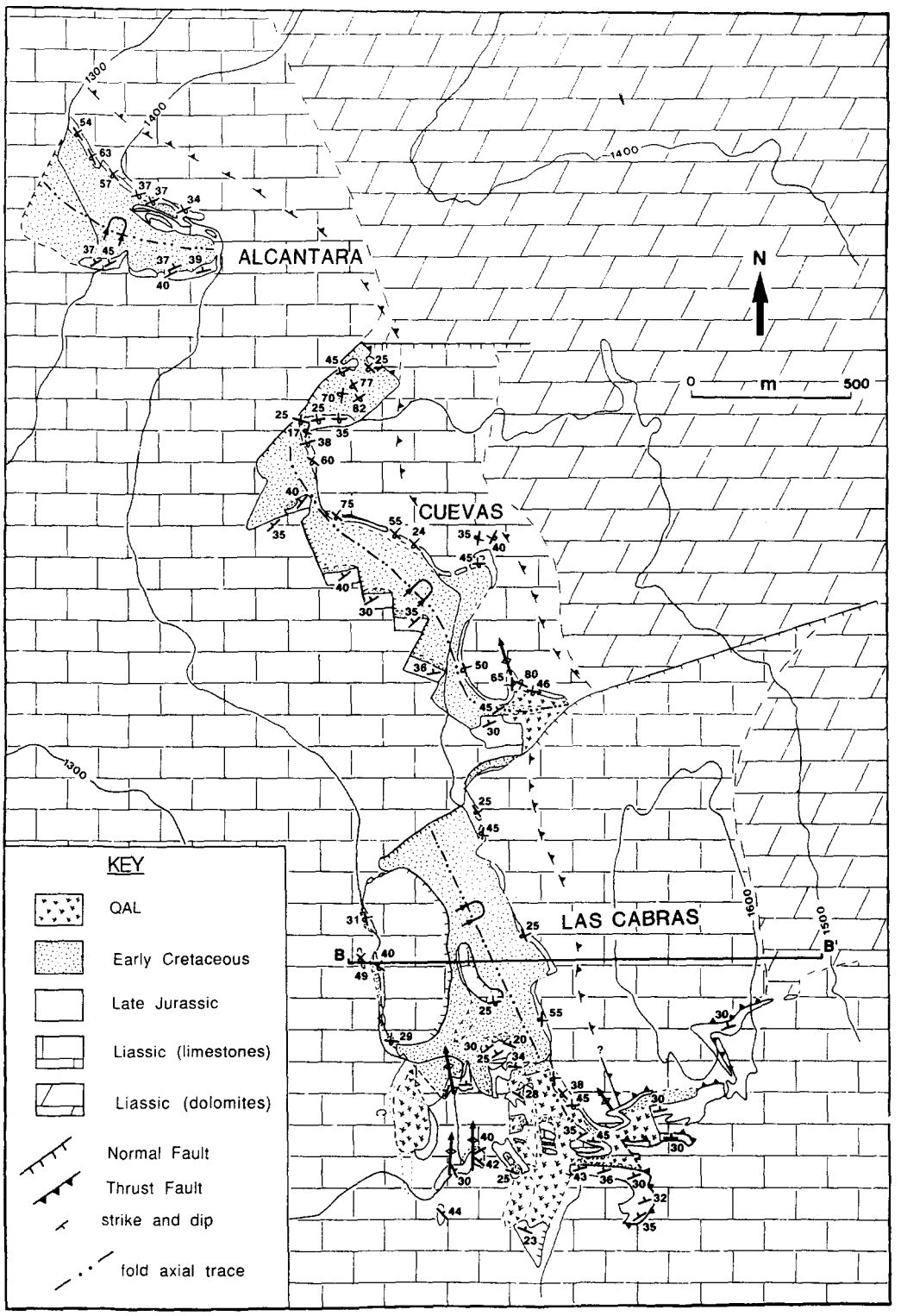


Fig. 3. Detailed geologic map of the three northern exposures of Late Jurassic to Cretaceous rocks which crop out along the axial fault zone (A). Location of this area is shown in Fig. 1.

thrusting (N40°E) form the northern and southern boundaries of the three exposures. These faults appear to displace both the footwall syncline and the thrust fault sequentially downward to the south. In addition to faults, parasitic folds on a variety of scales also occur, some of which are overturned in the direction of thrusting. They can be observed clearly in the normal limb of the Las Cabras exposure (Fig. 3).

It is the interaction between the topography and the ≈30° northward-dipping, overturned syncline, which has been affected by high-angle normal faulting, that results in the outcrop pattern in the three northern exposures of Late Jurassic and Cretaceous rocks (Fig. 3). Along the N–S-trending sections of these exposures (for example, along the central parts of the Cuevas and the Las Cabras exposures, Fig. 3), both the reverse and normal flanks of the syncline are observed. In contrast, along the E–W-trending sections such as the Alcantara

exposure, and the northern and southern boundaries of the Cuevas and the Las Cabras exposures, the hinge area of the regional syncline crops out.

*Early folds*

According to the most recent publication on the region (Instituto Geologico y Minero de España (IGME) 1989), the structure of the Sierra Gorda results from the superposition of two tectonic phases: an early phase that produced the folds in the axial zone trending N150°E, and a later phase of open folding with axes trending N30°–50°E. Since the thrusts are related to the folds in the axial zones, IGME's (1989) order implies that the main thrust surface along with its kinematic indicators should be folded about the later set of axes. The results of this study show (Figs. 2 and 3), however, that neither the kinematic indicators nor the surfaces along which thrusting occurred have been folded. This suggests that the open folds (N30°–50°E) must have formed before the thrust sheets. An early phase of open folding also explains the original northward dip of the sedimentary layers in the three northern exposures.

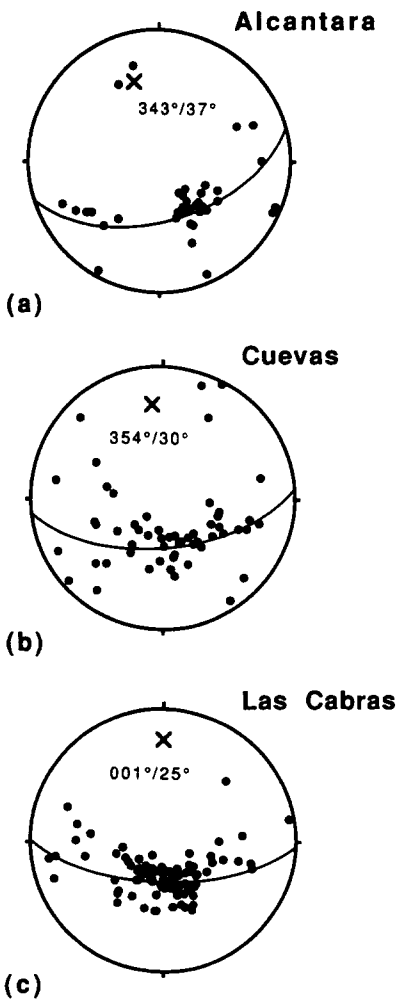


Fig. 4. Equal-area plots of the poles to bedding for the three Late Jurassic to Cretaceous exposures in Fig. 3. These plots show that the bedding is folded about an axis which is plunging approximately 30° to the north.

## PALAEOMAGNETIC AND ROCK MAGNETIC METHODS

In this study 10–14 cores were collected per site from six to 14 beds spread over an area dependent on the specific lithology. Samples were collected using a portable drill, and oriented with a Brunton compass and an orienting platform. The pelagic limestones sampled in this study were weakly magnetized and so did not significantly affect these orienting procedures. Standard cylindrical cores of 2.5 cm diameter and 10 cm length were later drilled and cut in the laboratory into 2.25 cm length samples. Generally one sample per core was demagnetized.

In the laboratory the samples were carefully analyzed to isolate the stable characteristic component of remanent magnetization (ChRM), to establish the magnetic properties of the sediments and to characterize the minerals responsible for the magnetization of the rock.

To isolate the primary component of magnetization, stepwise thermal demagnetization procedures were used. During the thermal demagnetization procedure each sample was demagnetized with a minimum of 10 steps based on a scheme designed after a detailed pilot demagnetization study. For this procedure a Schonstedt Thermal Demagnetizer with a rest field of approximately 10 nT was used. Measurement of the natural remanent magnetization (NRM) of the samples was done on a three axis ScT cryogenic magnetometer (Goree & Fuller 1976). On a set of representative samples bulk susceptibility was measured between each thermal demagnetization step on a KLY-1 susceptibility bridge.

Isothermal remanent magnetization (IRM) experiments, performed on a representative number (≈13), were used to characterize the properties of the magnetic carriers and thereby to determine the magnetic mineralogy of the sediments. Acquisition experiments were conducted at room temperature using an electromagnet with a maximum field strength of 1.1 T. As a final step, to examine the change in the direction of magnetization due to the rotation of the low coercivity minerals, the samples were placed in a field of 0.05 T along an axis normal to the previously defined axis. Subsequent thermal demagnetization of the two component IRM gave the thermal decay history of both the high and the low coercivity component of magnetization.

In addition to the above described procedures, anisotropy of magnetic susceptibility (AMS) was measured on a select group of sites with a Digico Anisotropy Delineator Spinner Magnetometer (Schultz-Krutisch & Heller 1985). The purpose of these experiments was to ascertain if the sediments had acquired a magnetic fabric. Fabric development in sediments is often the result of bulk strains imposed on the sediment. This deformation frequently occurs either during compaction of the sedimentary layer and results in a sedimentary fabric or during a tectonic event such as the Alpine orogeny and results in a tectonic fabric which may distort the natural remanent magnetization (NRM) directions.

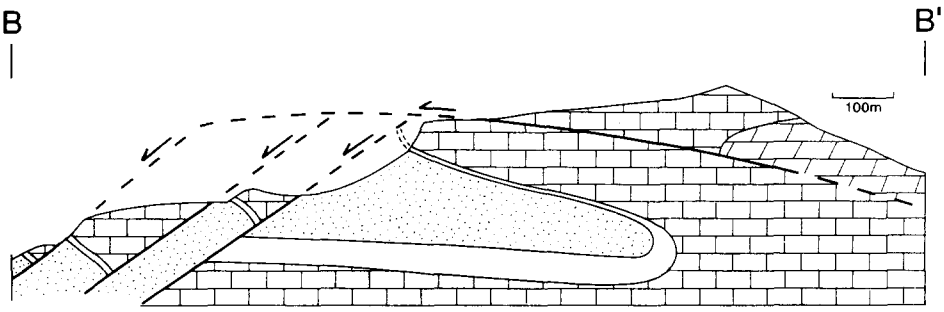


Fig. 5. E–W cross-section along line B–B′ in Fig. 3 constructed in a section plane dipping 60° south.

## PALAEOMAGNETIC AND ROCK MAGNETIC RESULTS

Palaeomagnetic samples for this study were cored at two early Jurassic, seven Late Jurassic, one Late Cretaceous site and two Miocene sites (Fig. 6 and Table 1). Five of the seven Late Jurassic sites and the one Late Cretaceous site were sampled along the eastern edge of the Sierra Gorda. One Late Jurassic site was cored in the normal stratigraphic sequence that crops out within the axial zone of the range. The Miocene localities were sampled in the Tortonian lacustrian limestones of the Granada basin. The remaining three sites, one Late Jurassic and two Early Jurassic, were sampled in the adjacent Subbetic unit to the west of the Sierra Gorda.

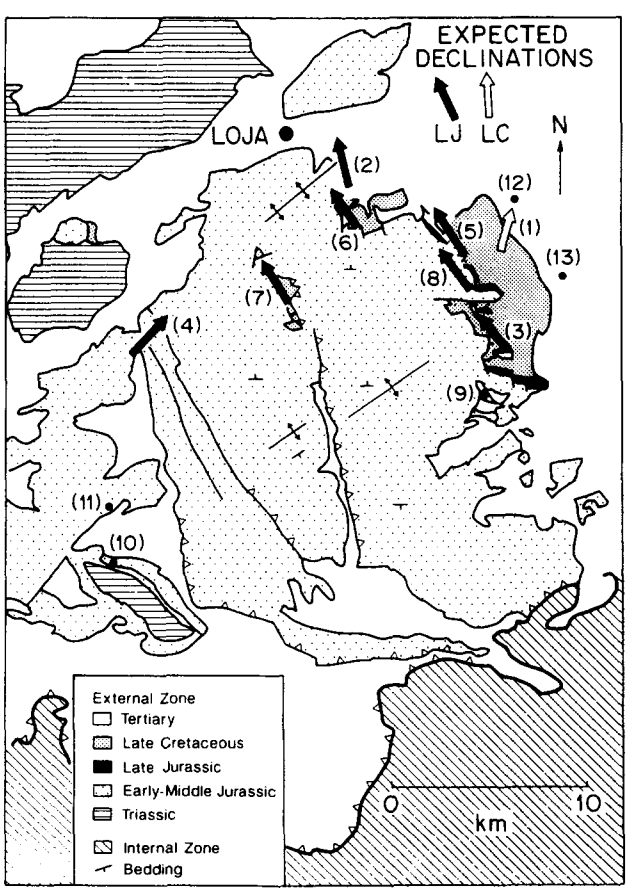


Fig. 6. Palaeodeclination map of site means from the Sierra Gorda. LJ—Late Jurassic, LC—Late Cretaceous. Expected declinations calculated from Westphal *et al.* (1986). Numbers correspond to locations as indicated on Table 1. Bedding dip direction is indicated in Jurassic sediments.

The Early Jurassic sites cored to the west of the Sierra Gorda and the Miocene sites proved unusable for palaeomagnetic study. Both of these limestones units are weakly magnetized and as a result do not yield a stable direction of ChRM.

In contrast to the Early Jurassic limestones, the magnetic properties of the Late Jurassic *Ammonitico rosso* limestones make them superb remanence carriers. Isothermal remanent magnetization (IRM) acquisition curves show a large low coercivity fraction which begins to saturate in fields of 0.1 T and then a gradual climb (Fig. 7a). The thermal demagnetization of a two-component IRM (Fig. 7b) shows mainly decay of the low coercivity fraction up to 525°C. The relatively low blocking temperature suggests that the magnetization in these samples is carried by a titano-magnetite. In general, any magnetization that may remain in the samples after they are heated above 600°C is negligible. This indicates that the high coercivity mineral phase observed in the IRM acquisition curves may be pigmentary hematite, which is either superparamagnetic or is unblocked at temperatures below 600°C. In some cases the high coercivity mineral is unblocked at temperatures higher than 600°C. In these cases the magnetic carrier is most likely coarse-grained specular hematite.

The natural remanent magnetization (NRM) of the Late Jurassic *Ammonitico rosso* limestones has an intensity around $8 \times 10^{-3}$ A m$^{-1}$ and a direction that scatters around a mean near the present field direction (351° declination, 53° inclination) before tectonic tilt correction. Thermal demagnetization of the NRM to temperatures around 350°C (Fig. 8) proved effective in removing this present field overprint. An intermediate component corresponding to the Neogene remagnetization reported by Villalaín *et al.* (1992) was not isolated. At temperatures above 350–400°C the magnetic vector in many samples began to decay linearly to the origin of the Zijderveld plot. Stable characteristic directions were usually obtained between 400 and 600°C. This higher temperature component shows both normal and reverse polarity and has been correlated by Ogg *et al.* (1984) to the Upper Jurassic marine magnetic anomaly record, suggesting that this component is most probably Upper Jurassic in age. Figure 8 shows examples of typical vector diagrams for these Late Jurassic limestones.

The characteristic component of the remanent magnetization in Jurassic limestones of the Sierra Gorda has

Table 1. Remanent magnetization parameters

| Sites used in this study Location | Site | $n$ | Age | Lat°N/Long°W | $Dec_{(b)}$ | $Inc_{(b)}$ | $\alpha_{95}$ | $k$ | $Dec_{(a)}$ | $Inc_{(a)}$ | $\alpha_{95}$ | $k$ | dip/dir |
|---|---|---|---|---|---|---|---|---|---|---|---|---|---|
| 1 | LC01 | 7 | LC | 37.1/4.1 | 202.1 | 17.3 | 42.4 | 3.5 | 8.6 | 49.8 | 6.3 | 113.2 | 60/225 |
| 2 | LJ01 | 11 | LJ | 37.2/4.1 | 320.4 | 47.5 | 3.3 | 190.0 | 354.8 | 37.8 | 3.0 | 255.3 | 27/042 |
| 3 | LJ03 | 9 | LJ | 37.0/4.0 | 289.4 | 41.8 | 9.3 | 31.5 | 317.6 | 36.2 | 9.4 | 31.0 | 34/024 |
| 4 | LJ04 | 7 | LJ | 37.1/4.2 | 17.9 | 31.0 | 6.0 | 101.6 | 42.6 | 54.2 | 6.0 | 101.6 | 35/161 |
| 5 | LJ05 | 7 | LJ | 37.1/4.1 | 304.3 | 43.1 | 10.5 | 28.5 | 332.0 | 34.7 | 10.6 | 28.5 | 28/343 |
| 6 | LJ06 | 8 | LJ | 37.1/4.1 | 317.5 | 55.8 | 10.7 | 27.6 | 326.6 | 30.3 | 11.2 | 25.6 | 34/343 |
| 7 | LJ09 | 12 | LJ | 37.1/4.2 | 318.5 | 73.2 | 9.3 | 22.7 | 326.3 | 45.5 | 8.4 | 28.0 | 20/333 |
| 8 | Ogg 84 | 97 | LJ | 37.2/4.1 | | | | | 323.2 | 30.0 | 2.5 | 34.7 | 36.0 |

| Sites not used in this study Location | Site | $n$ | Age | Lat°N/Long°W | $Dec_{(b)}$ | $Inc_{(b)}$ | $\alpha_{95}$ | $k$ | Comments | dip° |
|---|---|---|---|---|---|---|---|---|---|---|
| 9 | LJ02 | 9 | LJ | 37.0/4.0 | 77.2 | 53.9 | 32.1 | 3.5 | low intensity | 20.0 |
| 10 | LJ07 | 5 | EJ | 36.9/4.2 | 42.4 | 67.3 | 38.1 | 4.0 | low intensity | 41.0 |
| 11 | LJ08 | | EJ | 37.0/4.2 | | | | | low intensity | 10.0 |
| 12 | LM0110 | | TM | 37.1/4.0 | 321.3 | 17.7 | 35.5 | 2.8 | low intensity | 9.0 |
| 13 | LM02 | | TM | 37.1/4.0 | | | | | low intensity | 20.0 |

*$N$ is the total number of sites. Column 1 gives locations (loc.) which correspond to Fig. 3. Columns 2–14 give the site name, number of samples used per site ($n$), age of the outcrop (EJ—Early Jurassic, LJ—Late Jurassic, LC—Late Cretaceous, TM—Miocene), latitude and longitude of the site, declination (DEC), inclination (INC), $k$ and the circle of confidence $\alpha_{95}$; subscripts (b) and (a) indicate before and after tectonic tilt correction. dip—average dip of the bedding, and dir—dip direction.

a mean direction of declination ($D$) = 328.3° ± 9.5°, inclination ($I$) = 36.0° ($\alpha_{95}$ = 7.8°, $k$ = 74.2) (Fig. 9). Unlike the Jurassic declinations observed elsewhere in the Subbetic (for example Osete *et al.* 1988, 1989, Platzman & Lowrie 1992) these directions are within the range expected for stable Iberia. An expected declination of 336° and inclination of 35° was calculated from the synthetic polar wander curve for Iberia (Wesphal *et al.* 1986). An $F$-ratio test of the Fischer precision parameters was applied to test the significance of the regional fold test. Site means from five to Late Jurassic sites sampled on the Sierra Gorda and one site mean from Ogg *et al.* (1984) were used (Table 1). The results of this test show that the mean direction is significantly improved after applying the tectonic tilt corrections. The ratio of the precision parameters is 6.03 which is greater than the critical value of the $F$-statistic (4.85) at the 99% confidence level.

The direction of the palaeomagnetic vector from site LJ04 (Fig. 6, location 4) which is a Late Jurassic *Ammonitico rosso* site located, across a fault, approximately 1 km west of the Sierra Gorda is declination ($D$) = 42.6°, inclination ($I$) = 54.2° ($\alpha_{95}$ = 6.0°, $k$ = 101.6). This direction is different from the other directions observed on the Sierra itself but is similar to Jurassic directions obtained further to the west (Platzman & Lowrie 1992).

Rock magnetic studies carried out on the one late Cretaceous site sampled in this area (Fig. 10) indicate the presence of both a low coercivity and a high coercivity mineral. The low coercivity mineral is unblocked by approximately 600°C and is probably magnetite. There is no high unblocking temperature mineral observed during the thermal demagnetization of the two-component IRM. This suggests that the higher coercivity phase may be a combination of goethite, which is demagnetized by 150°C and pigmentary hematite. Anisotropy of magnetic susceptibility (AMS) investigations indicates that the Late Cretaceous limestones do not have a well developed magnetic fabric.

The direction of the palaeomagnetic vector obtained at the Late Cretaceous site passes a fold test and has a mean declination of 8.6° ± 9.7. Although this is only one data point it is interesting that this site is rotated clockwise by approximately 40° from the mean Late Jurassic direction, a result which is consistent with a Late Cretaceous anticlockwise rotation of the Iberian Peninsula (Platzman & Lowrie 1992).

## CONCLUSIONS AND DISCUSSION

The Sierra Gorda is a thrust complex composed of three thrust sheets, which were stacked by westward directed thrusting that was superimposed on an earlier E–W-trending open fold structure. During the thrusting episode a tight overturned syncline trending N150°E was formed in the footwall of the upper thrust. There is no kinematic evidence for the southward-directed thrusting episode suggested by previous workers (Vera 1969, IGME 1989). The precise timing of the deformation is difficult to assess. However, because both the folding and thrusting events involve Oligocene sediments they must have occurred during or after the Oligocene.

Palaeomagnetic analysis shows that the average declination from sites on the uppermost thrust sheet have statistically the same direction as site LJ09 which is located on the thrust sheet below. This implies that displacement on these thrust surfaces did not result in differential rotation between the thrust sheets. Therefore, if rotation has occurred, it must have been the result of motion either along a deeper level thrust or along bounding strike-slip faults.

Unlike the palaeomagnetic data obtained from much of the external zones, data obtained from Sierra Gorda

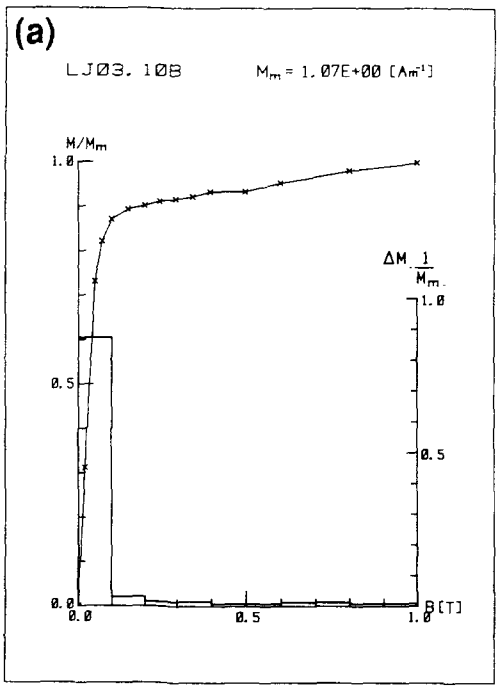


Fig. 7. (a) Isothermal remanent magnetization (IRM) acquisition curve and (b) vector diagram showing the thermal demagnetization behaviour of a two-component IRM, for a sample of late Jurassic *Ammonitico rosso* limestone.

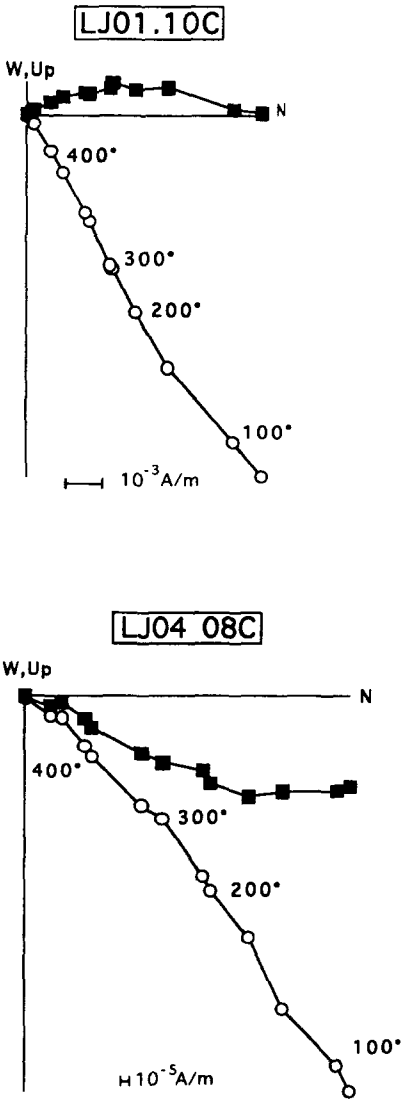


Fig. 8. Typical vector diagrams in geographic co-ordinates and corresponding unblocking temperature spectrum for two Late Jurassic carbonate samples undergoing thermal demagnetization. Squares represent vector end-points projected on the horizontal plane; circles are projections on the vertical N–S plane. Curves show that the NRM is composed of two components of remanent magnetization.

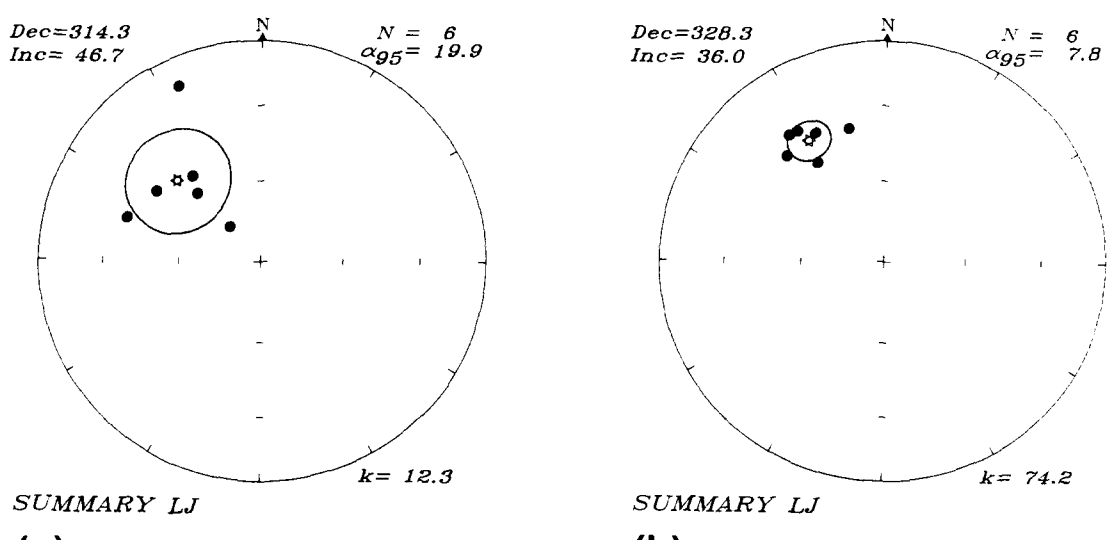


Fig. 9. Illustration of the regional fold test applied to the Jurassic limestones in the Sierra Gorda. Equal-area stereographic projection plots show the mean remanence vectors (a) before and (b) after tectonic tilt correction.

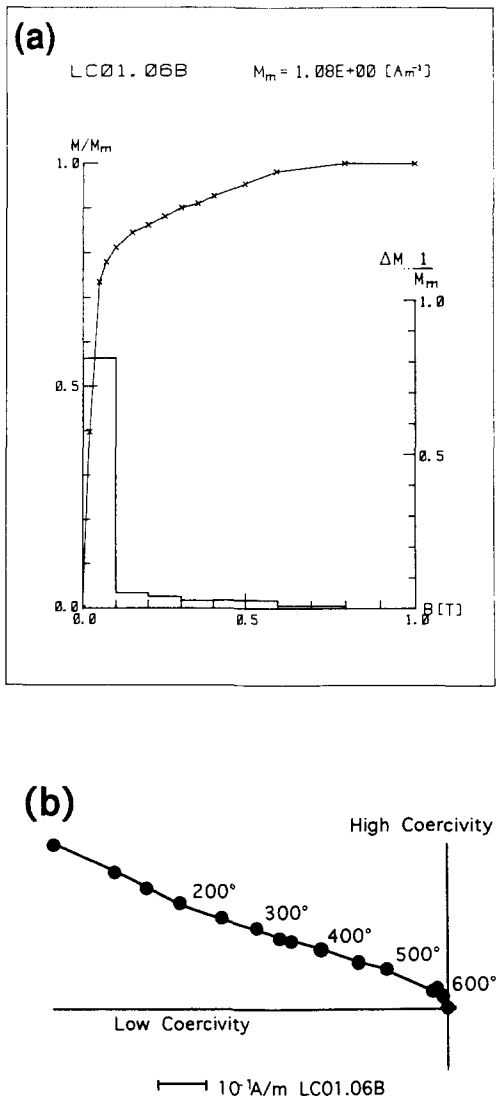


Fig. 10. (a) Isothermal remanent magnetization (IRM) acquisition curve and (b) vector diagram showing the thermal demagnetization behaviour of a two-component IRM, for a sample of Late Cretaceous *Capas rojas* marly limestone.

indicate that it is not rotated relative to stable Iberia. One possible hypothesis is that the Sierra Gorda experienced a clockwise rotation in concordance with the remainder of the Subbetic zone during the main Alpine tectonic event, but was then subsequently backrotated so as to exactly cancel the initial rotation. Osete *et al.* (1988) suggest that Late Miocene left-lateral motion on the North Betic Fault might have led to anticlockwise rotation of the Sierra Gorda. Although the Sierra Gorda has not rotated anticlockwise relative to stable Iberia this explanation could still be used for a late Miocene backrotation. Alternatively, an anticlockwise rotation may have resulted from late orogenic pinning and back rotation of a thrust sheet. It has been shown above, however, that any backrotation probably occurred after the thrusting event which stacked the upper level thrust sheets of the Sierra Gorda.

An alternative and preferred explanation for the anomalous palaeomagnetic declinations is that the Sierra Gorda has never rotated with respect to stable Iberia. Platzman (1992) postulated that the palaeomagnetic determined rotations in the rest of the external Betic Cordillera might be a consequence of oblique convergence along an active NW–SE-trending Alboran margin. If, the apparent southerly step in the Internal–External zone boundary in this region reflects a pre-existing NNE–SSW-trending irregularity in the continental margin of the Alboran domain then the direction of convergence in the Sierra Gorda (ESE–WNW) would have been normal to the active margin. In this case, convergence would be orthogonal and block rotations would not be expected.

*Acknowledgements*—I wish to thank Professor W. Lowrie, Professor J. Ramsay, Professor F. Heller, Professor V. Garcia-Dueñas, Dr J. C. Balanya, Dr J. P. Platt and Dr R. Freeman for their help. This research was supported by a grant from the Swiss National Science Foundation (grant No. 20-5044.86).

## REFERENCES

Andrieux, J., Fontbote, J. M. & Mattauer, M. 1971. Sur un modèle explicatif de l'Arc de Gibraltar. *Earth Planet. Sci. Lett.* **12**, 191–198.

Banks, C. & Warburton, J. 1991. Mid-crustal detachment in the Betic cordillera of southeast Spain. *Tectonophysics*, **191**, 275–289.

Blumenthal, M. 1930. Sur les rapports des zones Subbétiques et Pénibétiques a hauteur d'Archidona–Alfarnate (Prov. de Malaga et de Granada). *C. r. Acad. Sci., Paris* **191**, 1018–1019.

Blumenthal, M. 1931. Géologie des chaines Pénibétiques et Subbétiques entre Antequerra et Loja, et des zones limitropheres (Andalousie). *Bull. Soc. géol. Fr.* **5**, 23–94.

Bouillin, J. P., Durand-Delga, J. & Olivier, P. 1986. Betic-Rifian and Tyrrhenian arcs: Distinctive features, genesis and development stages. In: *The Origin of Arcs* (edited by Wezel, F. C.). Elsevier, Amsterdam, 281–304.

de Smet, M. E. M. 1984. Wrenching in the external zone of the Betic Cordilleras, Southern Spain. *Tectonophysics* **107**, 57–79.

Frizon de Lamotte, D., Andrieux, J. & Guézou, J.-C. 1991. Cinématique des chévauchements néogène dans l'arc bético-rifain: discussion sur les modèles géodynamiques. *Bull. Soc. géol. Fr.* **4**, 611–626.

Garcia-Dueñas, V. & Martinez, J. M. 1988. Sobre el adelgazamiento mioceno del Dominio de Alborán, ei despegue exten. *Geogaceta* **5**, 53–55.

Garcia-Hernandez, M., Lopez-Garrido, R., Sanz de Galdeano, C. & Vera, J. A. 1980. Mesozoic paleogeographic evolution of the external zone of the Betic Cordillera. *Geologie Mijnb.* **59**, 155–168.

Garfunkel, Z. & Ron, H. 1985. Block rotations and deformation by strike-slip faults. The properties of a type of macroscopic deformation. *J. geophys. Res.*, **90**, 42–72.

Goree, W. S. & Fuller, M. D. 1976. Magnetometers using RF driven SQUIDS and their applications to rock magnetism and paleomagnetism. *Rev. Geophys. & Space Phys.* **14**, 592–608.

Hermes, J. J. 1988. The stratigraphy of the Subbetic and southern Prebetic of the Velez Rubio-Caravaca area and its bearing on transcurrent faulting in the Betic Cordilleras. *Proc. K. Ned. Akad. Wet.* **81**, 1–54.

Instituto Geologico y Minero de España. 1989. Mapa Geologici de España, 1:50,000. Loja (No. 1025).

Leblanc, D. & Olivier, P. 1984. Role of strike-slip faults in the Betic Rifian Orogeny. *Tectonophysics* **101**, 344–355.

Linares, A. & Vera, J.-A. 1966. Precisiones estratigráphicas sobre le serie Mesozoica de Sierra Gorda, Cordilleras Béticas (provincia de Granada). *Estud. Geol.* **12**, 69–99.

Lonergan, L., Platt, J. P. & Gallagher, L. In press. The Internal–External Zone Boundary in the eastern Betic Cordillera, S.E. Spain. *J. Struct. Geol.*

Marrett, R. & Allmendinger, R. W. 1990. Kinematic analysis of fault slip data. *J. Struct. Geol.* **12**, 973–986.

Ogg, J. G., Steiner, M. B., Oloriz, F. & Tavera, J. M. 1984. Jurassic magnetostratigraphy, 1. Kimmeridgian-Tithonian of Sierra Gorda and Carcabuey, southern Spain. *Earth Planet. Sci. Lett.* **71**, 147–162.

Osete, M. L., Freeman, R. & Vegas, R. 1988. Preliminary paleomagnetic results from the Subbetic Zone (Betic Cordillera, Southern

Spain): Kinematic and structural implications. *Phys. Earth & Planet. Interiors*, **52**, 283–300.

Osete, M. L., Freeman, R. & Vegas, R. 1989. Paleomagnetic evidence for block rotations and distributed deformation of the Iberian–African plate boundary. In *Paleomagnetic Rotations and Continental Deformation, Volume* 254 (edited by Kissel, C. & Laj, C.). Kluwer, London, 381–385.

Paquet, J. 1972. Charriages et coilissements dans l'Est des Cordillères Bétiques (Espagne). *Proc. 24th Int. Geol. Cong.* **3**, 295–404.

Platt, J. P., Leggett, J. K. & Alam, S. 1988. Slip vector and fault mechanics in the Makran accretionary wedge, southwest Pakistan. *J. geophys. Res.* **93**, 7955–7973.

Platt, J. P. & Vissers, R. L. M. 1989. Extensional collapse of thickened continental lithosphere: a working hypothesis for the Alboran Sea and Gibraltar Arc. *Geology* **17**, 540–543.

Platzman, E., Allerton, S., Platt, J. P. & Lonergan, L. 1991. Rotations along an obliquely converging margin: Betic Cordillera, SE Spain. *Eos* **72**, 127.

Platzman, E. S. 1992. Paleomagnetic rotations and kinematics of the Gibraltar Arc. *Geology* **20**, 311–314.

Platzman, E. S. & Lowrie, W. S. 1992. Paleomagnetic evidence for the rotation of the Iberian Peninsula and the External Betic cordillera, Southern Spain. *Earth Planet. Sci. Lett.* **108**, 45–60.

Schultz-Krutisch, T. & Heller, F. 1985. Comparative measurements of magnetic susceptibility anisotropy in red sandstones. *Phys. Earth & Planet. Interiors* **51**, 320–325.

Twiss, R. J., Protzman, G. M. & Hurst, S. D. 1991. Theory of slickenline patterns based on the velocity gradient tensor and microrotation. *Tectonophysics* **186**, 215–239.

Vera, J. A. 1969. Estudio Geológico de la Zona Subbética en la transversal de Loja y sectores adyacentes. *Mem. I.G.M.E.* **82**, 1–192.

Villalaín, J. J., Osete, M. L., Vegas, R. & Garcia-Dueñas, V. 1992. Nuevos resultados paleomagnéticos en el Subbético Interno, implicaciones tectónicas. *III Congr. Geol. España VIII Congr. Latinamericano de Geologia* **1**, 308–312.

Westphal, M., Bazhenov, M. L., Lauer, J. P., Pechersky, D. M. & Sibuet, J. C. 1986. Paleomagnetic implications on the evolution of the Tethys belt from the Atlantic ocean to the Pamirs since the Triassic. *Tectonophysics* **123**, 37–82.